HYSTERETIC BEHAVIOR OF COMPACT STEEL BOX BEAM-COLUMNS

Iraj H. P. MAMAGHANI*, Tsutomu USAMI**, and Eiji MIZUNO ***

*Member of JSCE, Dr. of Eng., Research Associate, Dept. of Civil Eng., Kanazawa University
(Kodatsuno 2-40-20, Kanazawa 920, JAPAN)
**Fellow of JSCE, Dr. of Eng., Dr. SC., Professor, Dept. of Civil Eng., Nagoya University
(Chikusa-ku, Nagoya 464-01, JAPAN)
***Member of JSCE, Ph. D., Associate Professor, Dept. of Civil Eng., Nagoya University
(Chikusa-ku, Nagoya 464-01, JAPAN)

The present paper is concerned with the effect of some important parameters on the hysteretic behavior and energy absorption capacity of cantilever type compact steel box columns subjected to combined constant axial load and cyclic lateral displacement. The two-surface plasticity model, recently developed by the authors, is adopted for material nonlinearity in the finite element method used in the analysis. The main parameters concerned are: column slenderness ratio, axial load, steel grade and lateral load history. The effect of these parameters on the hysteretic behavior and energy absorption capacity is discussed and evaluated.

Key Words : column, structural steel, inelastic, hysteretic behavior, two-surface model

1. INTRODUCTION

With the rapid development of urban highway and bridge constructions, steel bridge piers of hollow box section have been widely designed and constructed in Japan. Although portal frame type piers are also used, the more popular type is the single pier of cantilever type which consumes less space. Since the performance of bridge piers under extreme loading conditions, such as severe earthquakes, is of great importance to prevent disruption of the urban transportation network, they must be designed to withstand such loading without collapse.

During the last few years a large number of experimental studies have been carried out to investigate the inelastic behavior of steel box beam-columns of cantilever type, modeling bridge piers, under the combined action of the dead load along the axial direction and the cyclic lateral loads arising from severe earthquakes[1)-4)]. However, an accurate analytical study of the hysteretic behavior of steel beam-columns has attracted limited attention[5)]. From the experimental studies, it was found that the main factors influencing the inelastic behavior of steel box beam-columns are the magnitude of the axial load, slenderness ratio parameters, width-to-thickness ratios of the plate components and cyclic mechanical properties of the material[2)]. Also, analytical and experimental investigations under monotonic loads revealed that strain hardening is very influential on the variation of ductility capacity of steel beam-columns, which is considered to be one of the most important parameter for evaluating the seismic performance of structures[6)].

On the other hand, energy absorption through hysteretic damping is one of the great interest in seismic design. Because it can reduce the amplitude of seismic response, and thereby, reduce the ductility demand on the structure. That is, further investigation is still needed to clarify the interaction effects of the steel grade (material properties, such as, yield plateau, Bauschinger effect and cyclic strain hardening), loading history and structural parameters on the hysteretic behavior and energy absorption capacity of the steel box beam-columns under cyclic loads.

The present paper is concerned with the cyclic inelastic large displacement behavior of compact steel box beam-columns of cantilever type. Here, "compact" means that no local buckling effect need not be taken into consideration. An

elastoplastic finite element formulation for beam-columns, considering geometrical and material nonlinearities, was coded and implemented in the computer program FEAP[7] used in the analysis. The two-surface plasticity model[8),9)] (2SM), was adopted for material nonlinearity.

The developed formulation accounts for the cyclic behavior of structural steels within the yield plateau, Bauschinger effect, cyclic strain hardening as well as gradual variation of section properties in line with the spread of plasticity across the section and along the member length.

The proposed approach has the advantage of avoidance of generating the moment-curvature curve required in the lump plasticity method of analysis. The cyclic plasticity performance of the formulation was examined by comparing with experiments and other models[10)-12)] . It was found that the proposed beam-column formulation can predict with a high degree of accuracy the experimentally observed cyclic behavior of steel box columns.

In this paper, the developed formulation is used to investigate the effect of some important parameters on the hysteretic behavior and energy absorption capacity of steel beam-columns of compact box section. A series of numerical experiments on hypothetical specimens are carried out to study the cyclic behavior of cantilever type steel box columns subjected to combined constant axial load and cyclic lateral displacement.

The main parameters considered are: (1) Column slenderness ratio, $\bar{\lambda}$; (2) axial load; (3) steel grade; and (4) lateral load history. Four values of $\bar{\lambda}$, namely, 0.2, 0.4, 0.6 and 0.8, and three values of P/P_y ratios (P_y = squash load of the column), namely, 0.0, 0.2 and 0.4 which are almost in the practical range are used. For each combination of $\bar{\lambda}$ and P/P_y, three materials , namely, SS400, SM490 and SM570, with material properties and corresponding two-surface model parameters given in Table 1[9)] , are assumed in the analysis. For each material, two type of lateral displacement histories, with constant and variable displacement amplitudes, are applied. The effect of these parameters on hysteretic behavior and energy absorption capacities are discussed and evaluated.

Table 1 Material properties and 2SM parameters for steel grades SS400, SM490 and SM570

Parameter	SS400	SM490	SM570
$E(GPa)$	206.7	205.8	215.6
$\sigma_y(MPa)$	274.4	357	524.3
ν	0.29	0.25	0.25
E^p_{st}/E	2.49×10^{-2}	3.40×10^{-2}	1.02×10^{-2}
ε^p_{st}	1.53×10^{-2}	1.24×10^{-2}	0.00
a	-0.505	-0.528	-0.553
b	2.17	1.88	6.47
c	14.4	18.7	34.8
α	0.191	0.217	0.175
e	5.00×10^{2}	3.16×10^{2}	7.00×10^{2}
f/E	0.30	0.484	0.361
M	-0.37	-0.522	—
E^p_0/E	8.96×10^{-3}	1.01×10^{-2}	7.85×10^{-3}
$\omega\cdot\sigma_y$	3.08	4.0	2.67
$\bar{\kappa}_0/\sigma_y$	1.15	1.13	1.06
σ_u/σ_y	1.81	1.61	1.22
$\zeta\cdot\varepsilon^2_y$	9.89×10^{-4}	1.52×10^{-3}	8.04×10^{-3}

2. METHOD OF ANALYSIS

An elasto-plastic analysis based on the finite element method[13)], using a conventional beam-column element of three displacements at each node, is employed in the analysis of compact steel columns. The analysis takes into account the spread of plasticity through the cross-section and along the length of member. In this approach, the member analyzed is divided into several beam-column elements along its length, and the cross-section is further subdivided into elemental areas, as shown in Fig. 1 for a hollow rectangular section. Each of the elemental areas is identified by, area dA_i, distance from the section centroid y_i, residual stress and strain, and stress-strain history. The incremental stress-strain relation for each elemental area is described by the 2SM[9)] .

In the present study, local buckling effect is not considered so that uniaxial stress-strain relationship (2SM) has been used in the analysis (multidimensional constitutive law is not needed). That is, only longitudinal stress (ε_x) is considered and so at any elemental area in the cross-section (see Fig. 1) yielding is assumed to occur as a result of longitudinal stress (σ_x) only. The stress resultants of axial force and bending moment are calculated simply by assuming the contribution of each elemental area over the cross-section[10)].

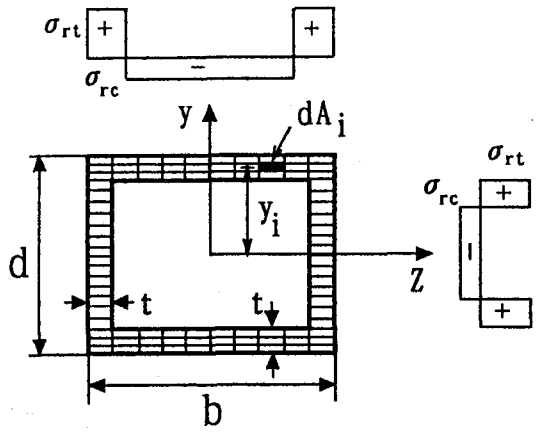

Fig. 1 Subdivision of section for a hollow rectangular section

The details of the element formulation for beam-column and the procedures of the numerical analysis can be found in the references 10) and 12). In what follows, the numerical results will be presented.

3. NUMERICAL RESULTS

The cyclic plasticity performance of the formulation was examined by comparing with experiments of several steel members, such as, pin-ended and fixed-ended columns of strut type[10] and steel box columns of cantilever type[11]. Also, using the 2SM, the predicted hysteretic behavior of experiments were compared with those obtained from elastic-perfectly plastic (EPP), kinematic hardening (KH) and isotropic hardening(IH) material models. The results have been presented in the authors previous papers in the references 10) – 12). It was found that the proposed beam-column formulation (2SM), can predict with a high degree of accuracy the experimentally observed cyclic behavior of steel members, both qualitatively and quantitatively, compared with the EPP, KH, and IH models[10)–12)]. Consequently, it was concluded that the use of EPP, KH and IH material models may lead to an erroneous estimate of hysteretic behavior of steel members in contrast to an accurate prediction by the 2SM. Also, it was found that the initial residual stress and an increase in the initial deflection significantly decrease the initial buckling load capacity and have almost no effect on the subsequent cyclic behavior of the column[11].

Based on the results of numerical experiments using the developed formulation (2SM), in what follows, the effect of some important parameters, such as, steel grade, column slenderness ratio and loading history, on the hysteretic behavior and energy absorption capacity of the steel beam-columns of compact box section will be presented and discussed.

3.1 Specimens

All of the assumed specimens have square box sections of size $b = 600\ mm$; and $t = 20\ mm$, as shown in Fig. 2.

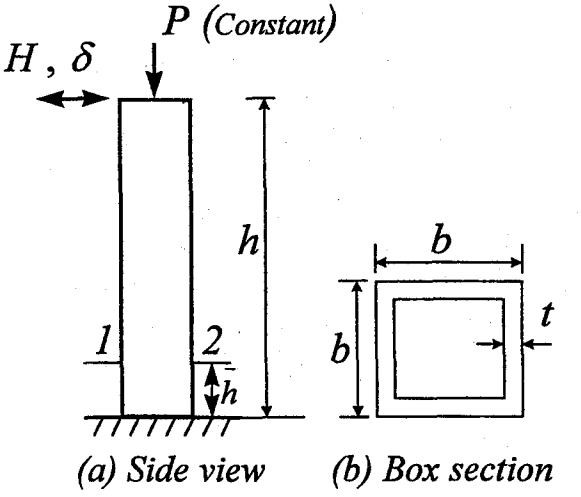

Fig. 2 Specimen

The height of each specimen h, is calculated using

$$\bar{\lambda} = \frac{Kh}{r}\frac{1}{\pi}\sqrt{\frac{\sigma_y}{E}} \qquad (1)$$

and corresponding parameters, in which h = height of the column; K = effective length factor; r = radius of gyration for the cross section; σ_y = yield stress; and E = Young's modulus.

3.2 Load sequences

After applying the prescribed constant axial load, lateral displacement histories which consists of fully reversed displacement cycles are applied. The lateral loading history of type 1 is described for 10 half-cycles with a constant peak displacement of $\delta/\delta_{y0} = \pm 4$ (see Eq. 3 for δ_{y0}). Whereas, in the loading history of type 2, the peak displacement is increased stepwise after three successive cycles at each displacement level; $\delta/\delta_{y0} = \pm 2, \pm 4$ and ± 6. In the analysis, each specimen is divided into ten elements along

its length and the cross section is subdivided into 8 and 17 layers, parallel to the axis of bending, for each flange and web, respectively. Initial geometrical imperfection, residual stress and local buckling are not considered. Also, based on the results of experiments[2], the axial strain is monitored in the outer most fiber of the cross section at point 1 near the base of the column (see Fig. 2; $\bar{h} = h/40$) where the stress reversals are severe, in order to check cyclic response of the material under different loading conditions. In what follows, some typical results will be presented and discussed.

3.3 Cyclic behavior

Figures 3(a) and 3(b) compare the normalized lateral load H/H_{y0}-lateral displacement δ/δ_{y0} and the normalized axial stress σ/σ_y-axial strain $\varepsilon/\varepsilon_y$ responses for specimens of $\bar{\lambda} = 0.4$ subjected to varying axial loads and lateral displacement of type 1, respectively. The notations H_{y0} and δ_{y0} indicate, respectively, the yield load and yield displacement (neglecting shear deformation) corresponding to zero axial load as follows

$$H_{y0} = \frac{M_y}{h} \tag{2}$$

and

$$\delta_{y0} = \frac{H_{y0}h^3}{3EI} \tag{3}$$

in which , M_y = yield moment; I = moment of inertia; and h = height of the column.

Figure 3(a) shows that the lateral load carrying capacity decreases as the axial load increases. Also, it can be observed that the stabilized state for the lateral load-displacement hysteresis loops is achieved after two cycles. The hysteresis loop become thinner after the first cycle and later it does not change significantly. The possible reasons for this behavior are: (1) The length of plastic zone stabilizes after the second cycle, because the yield plateau disappears and the material experiences cyclic strain hardening [thinning out of the hysteresis loops in Fig. 3(b)]. Consequently the spread of plasticity slows down and stabilizes; (2) the Bauschinger effect (reduction in the elastic range) of the material along the plastified zone, which causes the slope of hysteresis curves to decrease [consequently leading to a thinner hysteresis loops in Fig. 3(a)], is more apparent

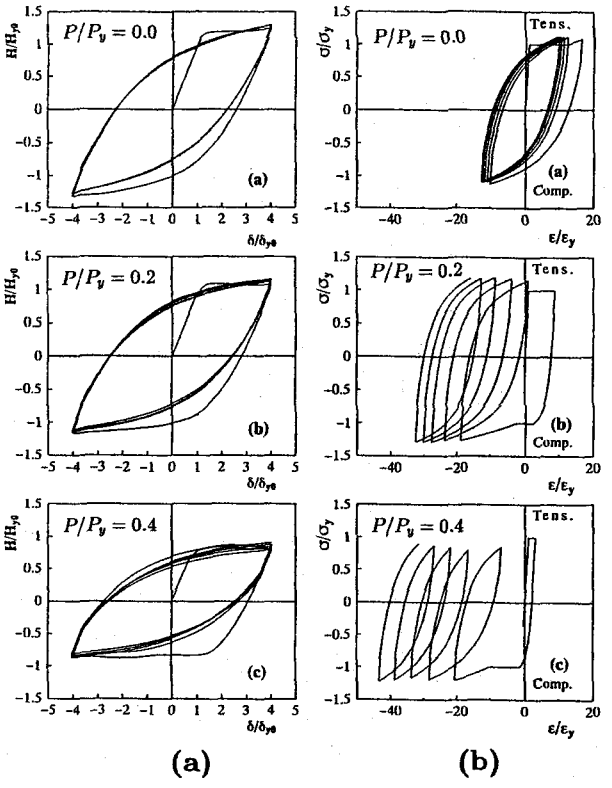

Fig. 3 Effect of axial load ($\bar{\lambda} = 0.4$, SS400): (a) normalized lateral load H/H_{y0}-lateral displacement δ/δ_{y0}; (b) normalized axial stress σ/σ_y-axial strain $\varepsilon/\varepsilon_y$ at point 1 ($\bar{h} = h/40$)

in the first two cycles than in the subsequent cycles, see Fig. 3(b). This effect is as a consequence of the larger rate of spread of plasticity in the first two cycles; and (3) since local buckling is not considered in the analyses, no degradation of the load carrying capacity is observed as the number of cycles increases.

Figure 3(b) shows that there is almost no accumulation of the inelastic axial strain (inelastic deformation) in the absence of the axial load ($P/P_y = 0.0$) due to cycling. Whereas, the axial strain increases in the direction of axial load (compression) due to lateral cycling under constant axial load (ratcheting effect), see Fig. 3(b) for $P/P_y = 0.2$ and $P/P_y = 0.4$. It is worth to note that similar behavior was observed from the experiment which was accurately simulated by the developed formulation (2SM)[11].

As shown in Fig. 3(b), the rate of ratcheting slows down as the number of cycles increases and the material experience cyclic strain hardening. Also, comparison between the results in Fig. 3(b) shows that the rate of ratcheting increases with the increase in axial load. This is an important

point, because the ratcheting phenomenon causes shortening of the plate components near the base of the column where the plastic deformation is large. Consequently, that may results a greater trend for local buckling to occur.

Figure 4 compares the effect of slenderness ratio parameter $\bar{\lambda}$, on the normalized lateral load H/H_{y0}-lateral displacement δ/δ_{y0} responses for specimens of steel grade SM490 subjected to lateral displacement of type 1 under constant axial load $P/P_y = 0.2$. The results in this figure show that as the slenderness ratio parameter increases, the load carrying capacity of the column decreases. The hysteretic loops stabilizes after two cycles under various slenderness ratio parameters (see Fig. 4).

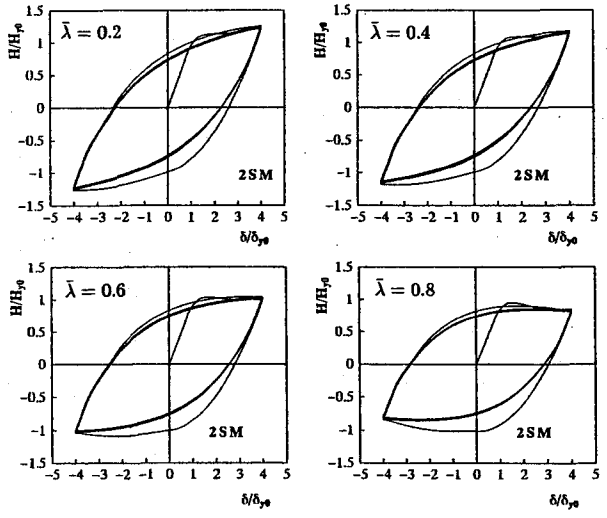

Fig. 4 Effect of slenderness ratio parameter ($P/P_y = 0.2$, SM490): normalized lateral load H/H_{y0}-lateral displacement δ/δ_{y0}

Figure 5(a) compares the normalized lateral load H/H_{y0}-lateral displacement δ/δ_{y0} responses for specimens of steel grade SM490 and SM570 subjected to lateral displacement of type 2 under constant axial load of $P/P_y = 0.2$. Fig. 5(b) illustrates the corresponding normalized axial stress σ/σ_y-axial strain $\varepsilon/\varepsilon_y$ responses at point 1 (see Fig. 2, $\bar{h} = h/40$). The main objective of these results is to compare the effect of steel grades and loading histories on the hysteretic behavior.

Comparison of the hysteresis loops in Fig. 5(a) shows that: (1) Degradation in load carrying capacity, for both steel grades, occurs when cycling is carried out within a small displacement range;

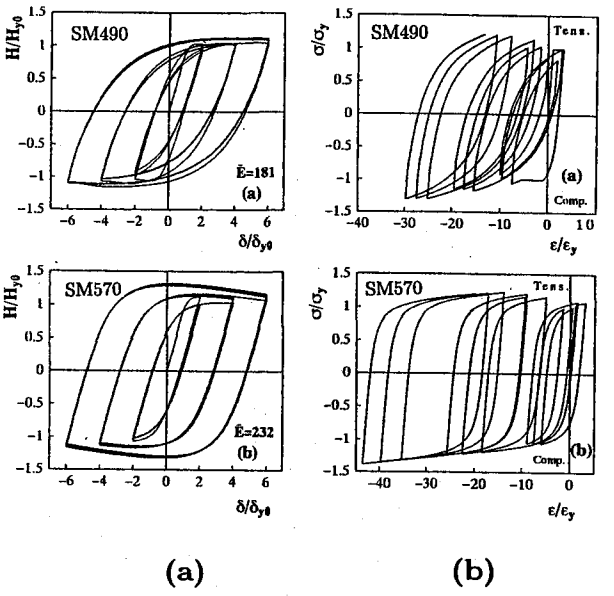

(a) (b)

Fig. 5 Effect of steel grade and loading history ($\bar{\lambda} = 0.6$, $P/P_y = 0.2$): (a) normalized lateral load H/H_{y0}-lateral displacement δ/δ_{y0}; (b) normalized axial stress σ/σ_y-axial strain $\varepsilon/\varepsilon_y$ at point 1 ($\bar{h} = h/40$)

$\delta/\delta_{y0} = \pm 2$; (2) stabilized state of the hysteresis loops is achieved after the second cycle for steel SM490, while the loops stabilize after the first cycle for steel SM570; and (3) the hysteresis loops are much fatter for SM570 than the corresponding ones for SM490.

All these observations may be mainly attributed to the reason that steel grade SM570 does not exhibit yield plateau in contrast to SM490, as can be noticed from Fig. 5(b) (see also Table 1 for material properties). The existence of the yield plateau causes a larger plastified zone in SM490 specimen compared to SM570, which in turn increases the Bauschinger effect. As a consequence, the hysteresis loops for steel SM490 become thinner.

Comparison of hysteresis loops in Fig. 5(b) indicates that the ratcheting effect is more apparent in the case of steel SM570 as a result of severe stress reversals. However, cyclic load carrying capacity does not degrade due to cyclic stain hardening, see Fig. 5(a) for SM570. In the second and third steps of loading, the hysteresis loops for the steel grade SM570 exhibit a larger descending behavior than that of the steel garde SM490 for which it is not so significant. This is, possibly, because of the larger ratchating effect

and further spread of plastic zone due to higher peak load in the case of SM570, see Fig. 5.

Figure 5(a) shows that the normalized cumulative energy absorption capacity (defined later) for steel grade SM490 ($\bar{E} = 181$) is 22 percent lower than that for the steel grade SM570 ($\bar{E} = 232$). This implies that the existence of yield plateau has a reducing effect on the normalized cumulative energy absorption capacity under the same loading history.

3.4 Energy absorption capacity

Energy absorption through hysteretic damping is of great interest in seismic design. Because it can reduce the ductility demand on the structures by reducing the amplitude of seismic response. In order to account for the loading history to which the inelastic performance of a structure is highly sensitive, a normalized energy absorption $\bar{E}$, defined as

$$\bar{E} = \frac{1}{E_{y0}} \sum_{i=1}^{n} E_i; \qquad (4)$$

$$E_{y0} = \frac{1}{2} H_{y0} \delta_{y0} \qquad (5)$$

is considered to be a more objective measure of the cyclic inelastic performance of a structure[2]. In Eq. 4, E_i =energy absorption in the i-th half-cycle, n = number of half-cycles (here, one half cycle is defined from any zero lateral load to the subsequent zero lateral load).

Using the above definitions, the results of numerical analysis regarding energy absorption capacity are summarized in Figs. 6-8 for the above discussed three steel grades, various $\bar{\lambda}$, P/P_y ratios and loading history of type 1. In what follows, it is aimed to illustrate the effect of these parameters on the energy absorption capacity under constant displacement amplitude cycling.

Figure 6 compares the normalized cumulative energy absorption capacity, $\bar{E}$ versus the number of half-cycles n, for steel grade SS400. It can be observed that all the curves corresponding to a specific P/P_y, say $P/P_y = 0.2$, and various $\bar{\lambda}$ almost coincide. It implies that the column slenderness parameter, $\bar{\lambda}$, has almost no effect on the normalized cumulative energy absorption capacity. Another observation from these results is that an increase in axial load P/P_y decreases the energy absorption capacity, especially when

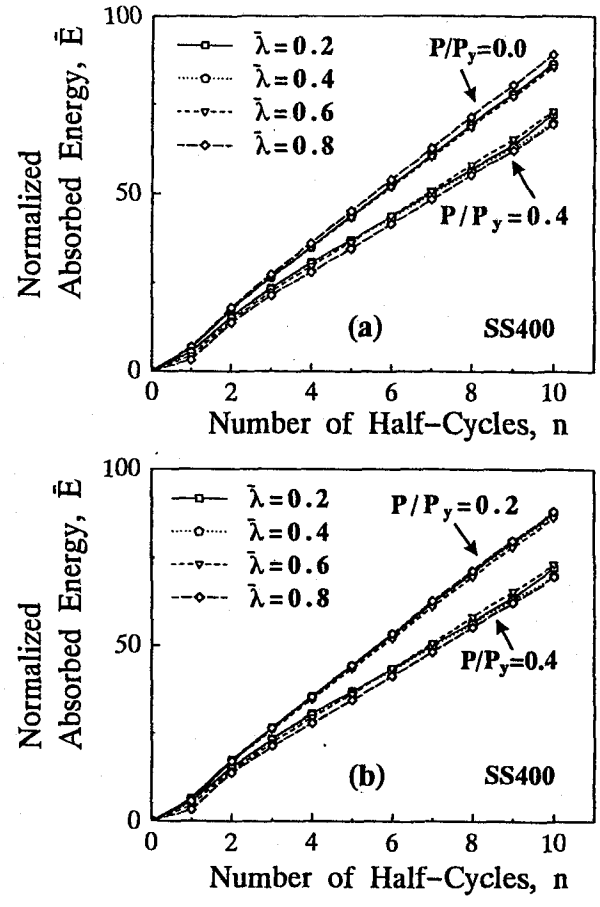

Fig. 6 Normalized energy absorption capacity $\bar{E}$-number of half-cycles n, for steel grade SS400

the number of cycles increases. However this effect is less predominant in case of $P/P_y \leq 0.2$, see Fig. 6. Similar results have been obtained for steel grades SM490 and SM570. However, the reduction of normalized energy absorption capacity due to increase in axial load is not so significant for steel grade SM570 (see Fig. 7).

As described before, the existence of yield plateau considerably reduces the stiffness of the column and affects the shape (thinning out) of hysteresis loops [see Figs. 5(a)], which in turns causes reduction in the normalized energy absorption capacity under the same loading condition.

Figures 7 and 8 compare the normalized energy absorption capacity for the steel grades SS400, SM490 and SM570. The results shown in these figures indicate that the normalize energy absorption capacities for steel grades SS400 and SM490 are very close to each other and are lower than that of steel grade SM570. The difference in normalized energy absorption capacities increases

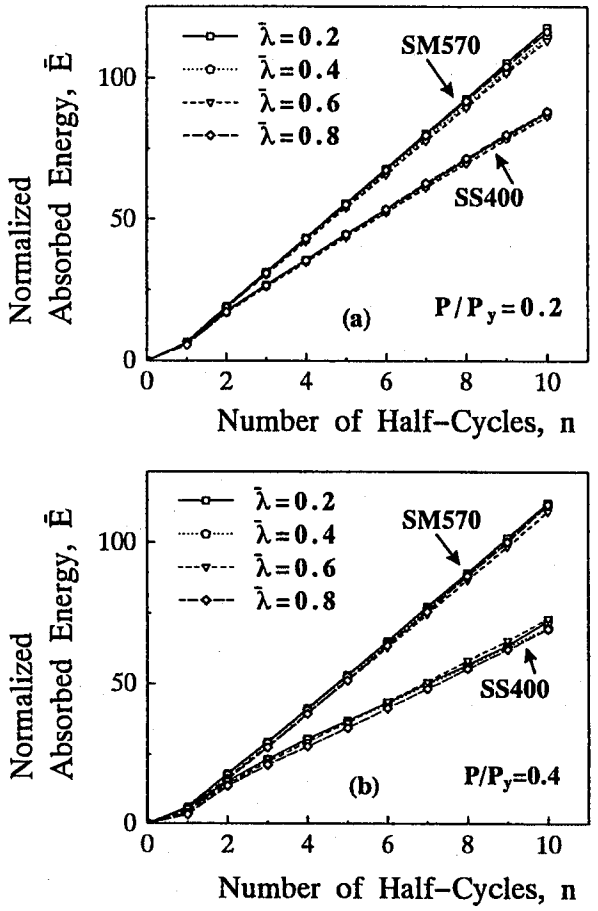

Fig. 7 Effect of steel grade and loading history: normalized energy absorption capacity $\bar{E}$-number of half-cycles n, for steel grades SS400 and SM570

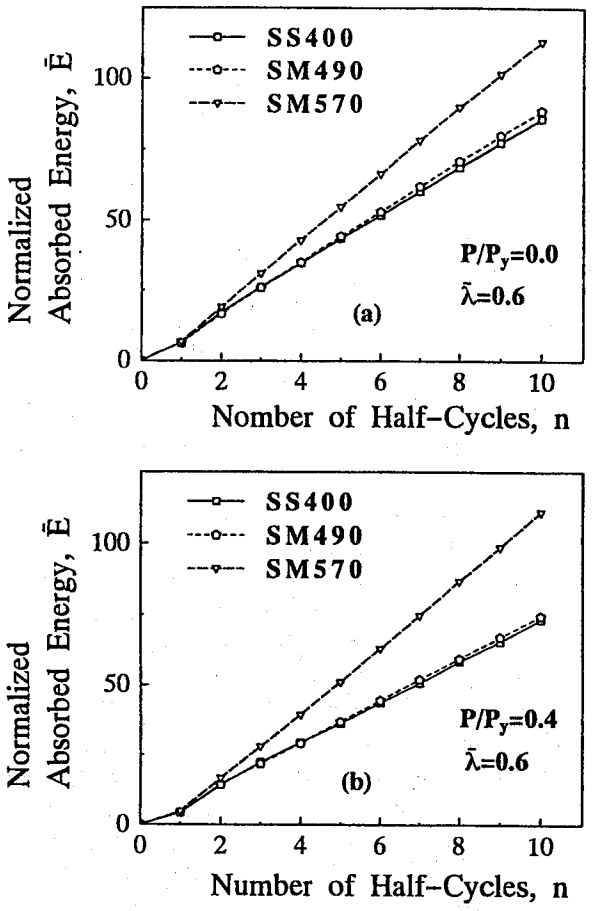

Fig. 8 Effect of steel grade: normalized energy absorption capacity $\bar{E}$-number of half-cycles n. (steel grades SS400, SM490 and SM570)

as the axial load and the number of cycles increases (see Figs. 7 and 8). These observations are mainly attributed to the fact that steel grades SS400 and SM490 exhibit yield plateau, while it is not the case for steel grade SM570.

4. CONCLUSIONS

The present paper was concerned with the cyclic inelastic large displacement analysis of compact steel box beam-columns of cantilever type. An elastoplastic finite element formulation for beam-columns, accounting for both the material and geometrical nonlinearities, used in the analysis. The two-surface plasticity model was employed for material nonlinearity.

Using the developed formulation, a series of parametric studies were carried out on steel box columns, and the effect of some important parameters, such as, column slenderness ratio, axial load, steel grade and lateral load history, on hysteretic behavior and energy absorption capacity were pointed out and evaluated. It was shown that: (1) The column slenderness parameter, $\bar{\lambda}$, has almost no significant effect on the normalized cumulative energy absorption capacity; (2) the stabilized state for the lateral load-displacement loops is achieved after two cycles in the absence of local buckling; (3) the yield plateau considerably affects the shape of hysteretic loops and has the effect of reducing the normalized energy absorption capacity; (4) the axial strain increases in the direction of axial load (compression) due to lateral cycling under constant axial load (ratcheting effect). Whereas, there is almost no accumulation of the inelastic axial strain in the absence of the axial load; and (5) the rate of ratcheting increases with the increase in axial load and it slows down as the number of cycles increases and the material experience cyclic strain hardening.

In this study no local buckling effect has been

considered, though it is extremely important when the behavior of steel bridge piers under severe earthquake loads is investigated. The research is now underway in Nagoya University.

REFERENCES

1) *Seismic Design WG Committee on New Technology for Steel Structures:* A Proposal for seismic design of steel bridges, JSCE, 1996.
2) Usami, T., Mizutani, T. Aoki, Itoh, Y.: Steel and concrete-filled steel compression members under cyclic loading, *Stability and ductility of steel structures under cyclic loading*, Edited by Fukumoto, Y. and Lee, G.C., CRC Press, Boca Raton, Fl, pp. 123-138, 1992.
3) Watanabe, E., and Dogaki, M.: The state of the art: Ductility and cyclic buckling- A Japanese contribution in the field of civil engineering, *Stability and ductility of steel structures under cyclic loading*, Edited by Fukumoto, Y. and Lee, G.C., CRC Press, Boca Raton, Fl, pp. 357-367, 1992.
4) Tominaga, T., and Yasunami, H.: An experimental study on ductility of steel bridge piers with thick walled cross section and small number of stiffeners, *Journal of Structural Engineering, JSCE*, Vol. 40A, pp. 189-200, March, 1994 (in Japanese).
5) Shaker, R.E., Murakawa, H., and Ueda, Y.: Effect of local buckling and work hardening properties of steel material on the behavior of I-beam subjected to lateral cyclic load, *Journal of Structural Engineering, JSCE*, Vol. 40A, pp. 121-134, March, 1994.
6) Nakashima, M.: Variation of ductility capacity of steel beam-columns, *Journal of structural Engineering, ASCE*, Vol. 120, No. 7, pp. 1941-1960, 1994.
7) Zienkiewicz, O. C.: *The finite element method, 3rd Ed.*, McGraw-Hill, New York, 1977.
8) Mamaghani, I. H. P., Shen, C., Mizuno, E. and Usami, T.: Cyclic behavior of structural steels. I: Experiments, *J. Engng Mech., ASCE*, Vol. 121(11), pp. 1158-1164, 1995.
9) Shen, C., Mamaghani, I. H. P., Mizuno, E. and Usami, T.: Cyclic behavior of structural steels. II: Theory, *J. Engng Mech., ASCE*, Vol. 121(11), pp. 1165-1172, 1995.
10) Mamaghani, I. H. P., Usami, T. and Mizuno, E.: Inelastic large deflection analysis of steel structural members under cyclic loading, *Engineering Structures*, UK, Vol. 18, No. 9, pp. 659-668, 1996.
11) Mamaghani, I. H. P., Usami, T. and Mizuno, E.: Cyclic elastoplastic large displacement behaviour of steel compression members, *Journal of Structural Engineering, JSCE*, Vol. 42A, pp. 135-145, March, 1996.
12) Mamaghani, I. H. P., Usami, T. and Mizuno, E.: Cyclic elastoplastic behavior of steel structures: Theory and experiment, *NUCE Research Report*, No. 9601, Nagoya Univ., Japan, 1996.
13) Clarke, M. J.: Plastic-zone analysis of frames, *Advanced analysis of steel frames*, Edited by Chen, W. F. and Toma, S., CRC Press, Boca Raton, Fl, pp. 259-319, 1994.

(Received on 18 September, 1996)